

The contribution of North Atlantic atmospheric circulation shifts to future wind speed projections for wind power over Europe

Article

Published Version

Creative Commons: Attribution-Noncommercial 4.0

Open Access

Gonzalez, P. L. M., Brayshaw, D. J. and Zappa, G. (2019) The contribution of North Atlantic atmospheric circulation shifts to future wind speed projections for wind power over Europe. *Climate Dynamics*. ISSN 1432-0894 doi: <https://doi.org/10.1007/s00382-019-04776-3> Available at <http://centaur.reading.ac.uk/83474/>

It is advisable to refer to the publisher's version if you intend to cite from the work. See [Guidance on citing](#).

To link to this article DOI: <http://dx.doi.org/10.1007/s00382-019-04776-3>

Publisher: Springer

All outputs in CentAUR are protected by Intellectual Property Rights law, including copyright law. Copyright and IPR is retained by the creators or other copyright holders. Terms and conditions for use of this material are defined in the [End User Agreement](#).

www.reading.ac.uk/centaur

CentAUR

Central Archive at the University of Reading

Reading's research outputs online



The contribution of North Atlantic atmospheric circulation shifts to future wind speed projections for wind power over Europe

Paula L. M. Gonzalez^{1,2} · David J. Brayshaw^{1,2} · Giuseppe Zappa¹

Received: 4 August 2018 / Accepted: 15 April 2019
© The Author(s) 2019

Abstract

Wind power accounts for a large portion of the European energy mix (17% of total power capacity). European power systems therefore have a significant-and growing-exposure to near-surface wind speed changes. Despite this, future changes in European wind climate remain relatively poorly studied (compared to, e.g., temperature or precipitation), and there is limited understanding of the differences shown by different general and regional circulation models (GCMs and RCMs). This study provides a step towards a process-based understanding of European wind speed changes by isolating the component associated with ‘large-scale’ atmospheric circulation changes in the CMIP5 simulations. The component associated with the large-scale atmospheric circulation is found to explain cold season windiness projections in the free troposphere over Western Europe, with the changes reflecting the poleward shift of the North Atlantic jet. However, in most GCMs the projected wind speed changes near the surface are more negative than would be expected from the large-scale circulation alone. Thus, while the spread in CMIP5 21st century near surface wind speed projections is associated with divergent projections for the large-scale atmospheric circulation, there is a remarkably good agreement concerning a relative reduction in near-surface wind speeds. This analysis suggests that projected 21st century wind speed changes over Western Europe are the result of two distinct processes. The first is associated with changes in the large-scale atmospheric circulation, while the second is likely to be more local in its connection to the near-surface boundary layer. An improved process-based understanding of both is needed for enhancing confidence in wind-power projections on multi-decadal timescales.

Keywords Climate change · Surface wind projections · North Atlantic modes of variability · Wind power generation · Western Europe

Electronic supplementary material The online version of this article (<https://doi.org/10.1007/s00382-019-04776-3>) contains supplementary material, which is available to authorized users.

✉ Paula L. M. Gonzalez
p.gonzalez@reading.ac.uk

David J. Brayshaw
d.j.brayshaw@reading.ac.uk

Giuseppe Zappa
g.zappa@reading.ac.uk

¹ Department of Meteorology, University of Reading, Reading, UK

² NCAS-Climate, University of Reading, Reading, UK

1 Introduction

Under the Europe 2030 Climate and Energy Strategy plan, the European Commission (EC) is aiming to reduce its greenhouse gas emissions in 40% with respect to 1990 levels and to produce 27% of its energy through renewable sources (EC 2013). Wind power generation is widely seen as an excellent resource to accomplish both goals, and has seen rapid increases in installed capacity in recent years (WindEurope 2018). In 2016, wind power accounted for around 17% of total power capacity in Europe.

Wind power is, however, strongly dependent on weather. As the lifetime of energy systems infrastructure (e.g., transmission lines and generation plants) is typically many decades, it is therefore important to accurately estimate how wind power resources may change over this period. In recent years, several authors have explored wind speed and wind power projections for Europe on the basis of GCM

simulations (e.g., Tobin et al. 2015, 2016; Reyers et al. 2016; Carvalho et al. 2017; Wohland et al. 2017; Karnauskas et al. 2018). Reyers et al. (2016) analyzed future projections from the latest Climate Model Intercomparison Project (CMIP5) ensemble and found an increase in wind energy potentials for winter over central and Northern Europe, though large differences between the model projections were noted. Tobin et al. (2015) found only weak changes in wind generation potentials for most of Europe, with the exception of robust decreases over the Mediterranean region. Wohland et al. (2017) found an increase in the likelihood of atmospheric circulation states associated with low wind over Europe. Carvalho et al. (2017), chose a sub-set of GCMs and concluded that wind power resources are likely to increase in central and Northern Europe and decrease in the Mediterranean region, though large model uncertainties were also found. Overall, a general pattern of wind speed change can be identified, associated with increases in Central and Northern Europe and decreases in Southern Europe.

It is well established from the recent historical period (i.e., covered by reanalysis) that large-scale slowly-varying atmospheric circulation patterns have a strong impact on European wind climate at seasonal to interannual scales, particularly over Western Europe (e.g., the North Atlantic Oscillation, East Atlantic, and Scandinavian patterns: Brayshaw et al. 2011; Ely et al. 2013; Zubieta et al. 2017, 2017). The projected northward shift and eastward extension of the North Atlantic jet and storm track into Europe under climate change (e.g., Ulbrich et al. 2009; Simpson et al. 2014; Zappa et al. 2015b) therefore appears to be somewhat consistent with the general pattern of wind changes mentioned above [see also Karnauskas et al. (2018)]. It is, however, important to note that GCM projections of the large-scale atmospheric circulation changes remain themselves uncertain, with large disagreements between GCMs to the extent that even the sign of the projected change is unclear over some regions. Moreover, the projected patterns of large-scale circulation change cannot be fully reconciled with the pattern of surface wind speed change: e.g., the projected ensemble mean UK surface wind speed change in CMIP5 is negligible, even though it lies in a region where the storm track change might be expected to increase surface wind speeds.

A further complexity arises from observationally-based studies of recent surface wind-speed trends, suggesting that local effects (in addition to changes in large-scale atmospheric circulation) may influence future surface windiness under climate change. In particular, a trend towards near-surface wind stilling in the Northern Hemisphere has been documented by several authors (e.g., Vautard et al. 2010; Bichet et al. 2012; Torralba et al. 2017). The cause of this trend remains unclear—with changes in both atmospheric circulation and land use (i.e., surface roughness) cited as potential contributors. Additionally, further uncertainties

might result from the differences in the model representation of boundary layer processes (e.g., Lindvall et al. 2013, 2017; Holtslag et al. 2013).

Two key messages therefore emerge from the literature. Firstly, that although some areas of agreement emerge in wind-speed projections (weak increases in Northern and Central Europe; decreases in the Mediterranean), there remain significant uncertainties due to GCM ensembles projecting different patterns of change in both surface winds and large-scale atmospheric circulation. Secondly, there is a poor understanding of the physical processes responsible for causing changes in near-surface wind climate.

Several studies have focused on isolating the effects of large-scale circulation changes on future projections for Europe (e.g., Deser et al. 2017; Kröner et al. 2017), but none have been applied to near-surface wind speed. The main objective of this study is therefore to evaluate the importance of changes in the North Atlantic atmospheric circulation for surface wind speed projections over Europe. An EOF- and regression-based technique is developed and used to identify the connection between the North Atlantic large-scale atmospheric circulation and European surface wind speeds over the historical period (Sect. 2.1), and the skill of CMIP5 GCMs in reproducing this connection is assessed (Sect. 3.1.2). The same technique is then used with the CMIP5 climate projections to isolate the component of surface wind-speed change associated with North Atlantic atmospheric circulation changes (Sect. 3.2), allowing this estimated component of the change to be compared to the GCM-based surface wind speed projections (Sect. 3.3). The paper concludes with a summary and discussion of open issues (Sect. 4).

2 Data and methodology

This study makes use of daily zonal and meridional wind components at 10 m, 850 hPa and 500 hPa. Two domains are considered in the analysis: an Atlantic–European domain (15N–75N, 80W–40E) to evaluate the large-scale atmospheric variability (associated with the North Atlantic jet), and a European domain (36N–70N, 11W–30E) to evaluate the ‘surface impacts’ relevant to wind-power applications. For the Atlantic–European domain, zonal wind at 850 hPa is processed using a 10-day Lanczos low-pass filter (Duchon 1979) to isolate the slowly varying component of the large-scale circulation.

Data is taken from two sources. Firstly, the ERA-Interim (ERA-I) Reanalysis (Dee et al. 2011) for the period 1979–2014, and secondly the CMIP5 general circulation model (GCM) ensemble (Taylor et al. 2012). For the CMIP5 data, two periods/experiments are considered: the recent historical period (1976–2005) and the

Table 1 CMIP5 GCMs considered in this study. Asterisks indicate that 10-m wind data was unavailable

Name	Modeling center	Atmospheric component	References
ACCESS1.0	CSIRO/BoM, Australia	UKMO UM 1.25°lat × 1.875° lon	Collier and Uhe (2012), Dix et al. (2013)
ACCESS1.3	CSIRO/BoM, Australia	UKMO UM 1.25°lat × 1.875° lon	Collier and Uhe (2012), Dix et al. (2013)
BCC-CSM1.1*	BCC, China	BCC AGCM2.1 2.7906°lat × 2.8125° lon	Wu et al. (2014)
BNU-ESM	BNU, China	Interim CAM4 2.7906°lat × 2.8125° lon	Ji et al. (2014)
CanESM2	CCCma, Canada	CanAM4 2.7906°lat × 2.8125° lon	Arora et al. (2011)
CMCC-CESM	CMCC, Italy	ECHAM5 3.4431°lat × 3.75° lon	Fogli et al. (2009)
CMCC-CM*	CMCC, Italy	ECHAM5 0.7484°lat × 0.75° lon	Scoccimarro et al. (2011)
CMCC-CMS	CMCC, Italy	ECHAM5 3.7111°lat × 3.75° lon	Manzini et al. (2006), Giorgetta et al. (2006)
CSIRO-Mk3.6.0	QCCCE/CSIRO, Australia	Mark3.6 1.8653°lat × 1.875° lon	Collier et al. (2011), Rotstayn et al. (2012)
EC-Earth*	EC-Earth Consortium, Europe	ARPEGE/IFS/ECMWF 1.1215°lat × 1.125° lon	Hazeleger et al. (2010, 2011)
FGOALS-G2*	LASG/IAP, China	GAMIL2 2.7906°lat × 2.8125° lon	Li et al. (2013)
GFDL-CM3	GFDL, USA	AM3 2°lat × 2.5° lon	Donner et al. (2011)
GFDL-ESM2G	GFDL, USA	AM2 2.0225°lat × 2° lon	Dunne et al. (2012)
GFDL-ESM2M	GFDL, USA	AM2 2.0225°lat × 2.5° lon	Dunne et al. (2012)
HadGEM2-CC	Hadley Center, UK	HadGAM2 1.25lat × 1.875 lon	Collins et al. (2011), Jones et al. (2011)
INM-CM4*	INM, Russia	1.5°lat × 2° lon	Volodin et al. (2010)
IPSL-CM5A-LR	IPSL, France	LMZ ₅ A 1.8947°lat × 3.75° lon	Dufresne et al. (2013)
IPSL-CM5A-LR	IPSL, France	LMZ ₅ A 1.2676°lat × 2.5° lon	Dufresne et al. (2013)
IPSL-CM5B-LR	IPSL, France	LMZ ₅ B 1.8947°lat × 3.75° lon	Dufresne et al. (2013)
MIROC-ESM	JAMSTEC, Japan	CCSR/NIES/FRCGC 2.7906°lat × 2.8125° lon	Watanabe et al. (2011)
MIROC-ESM-CHEM	JAMSTEC, Japan	CCSR/NIES/FRCGC 2.7906°lat × 2.8125° lon	Watanabe et al. (2011)
MIROC5	JAMSTEC, Japan	CCSR/NIES/FRCGC 1.4008lat × 1.4062 lon	Watanabe et al. (2011)
MPI-ESM-LR	MPI-M, Germany	ECHAM6 1.8653°lat × 1.875° lon	Giorgetta et al. (2013)
MPI-ESM-MR	MPI-M, Germany	ECHAM6 1.8653°lat × 1.875° lon	Giorgetta et al. (2013)
MRI-CGCM3	MRI, Japan	MRI-AGCM3 1.1215°lat × 1.125° lon	Yukimoto et al. (2012)
NorESM1-M*	NCC, Norway	CAM4-Oslo 1.8947°lat × 2.5° lon	Tjiputra et al. (2012), Bentsen et al. (2013)

high-emissions RCP8.5 future scenario (2070–2099). The climate change response is evaluated as the difference between the climatologies of the two periods. The choice for the most extreme future scenario and the future period at the end of the century is meant to maximize signal-to-noise ratio and allow for a better estimation of the projected changes. This is necessary given that prior studies found that wind changes projected by these models over Europe tend to be of small amplitude compared with internal variability (e.g., Carvalho et al. 2017). A single ensemble member from each of the 26 CMIP5 GCMs listed in Table 1 is considered. In the cases where the multi-model means (MMM) are presented, each individual GCM is first interpolated to the grid of the ERA-I reanalysis. It is also noted that only 20 of the 26 CMIP5 models had daily 10-m wind data available (see Table 1). To maximize the data available to the analysis, individual results from each of the 26 models are presented whenever it is possible to do

so. However, for multi-model means, only the 20 models with 10-m wind data are used. This is done to enable direct comparisons between signals obtained at different vertical levels (i.e., the common 20 GCMs are used to build the MMM results for 10 m, 850 hPa and 500 hPa).

Following Zappa et al. (2015b), two extended seasons are defined: a cold season from November to April and a warm season from May to October. This choice maximizes the signal to noise ratio in the climate response, by capturing the seasonality in the projected circulation response over Europe while reducing the noise due to internal variability compared to meteorological seasons. Seasonal statistics will refer to averages over these two periods in the rest of the manuscript. The seasonal North Atlantic Oscillation (NAO) and East Atlantic (EA) pattern indices used in Sect. 3.1.1 are calculated by NOAA/CPC following the method of Barnston and Livezey (1987) and are publicly available through the IRI Data Library (Blumenthal et al. 2014).

2.1 Estimating the wind associated with the large-scale modes of variability

To isolate the variability of near-surface wind over Europe linked to the North Atlantic atmospheric circulation, the leading modes of variability of 10-day low-pass daily filtered zonal wind (\tilde{u}) at 850 hPa in the Euro-Atlantic domain are considered. These modes are identified for each season through an empirical orthogonal functions (EOF) analysis. The percent of variance associated with each EOF and their accumulation is used to decide how many modes to retain (in each case 2 EOFs are retained, see Sect. 3.1.1).

A multiple linear regression (MLR) model is then constructed,¹ linking the principal component (PC) time series corresponding to the retained EOFs to the wind speed at each vertical level over the European domain, for the ERA-I reanalysis and for each individual CMIP5 historical simulation. The MLR is constructed separately for each grid point, for each season (NDJFMA and MJJASO) and for each vertical level (10 m, 850 hPa and 500 hPa). Once the MLR is established, it is possible to derive an estimate of the wind speed over the European domain based only on the PCs representing the large-scale circulation over the Atlantic-European domain. This is referred to as the wind speed ‘estimation’, as compared to the gridded wind speed data from the GCM or reanalysis output. The estimation technique is hereafter referred to as EOF-MLR and is described by :

$$\widehat{ws}^{hist}(x, y, z, t) = A(x, y, z).PC1^{hist}(t) + B(x, y, z).PC2^{hist}(t) + C(x, y, z), \quad (1)$$

where \widehat{ws}^{hist} represents the estimated historical wind speed, $PC1$ and $PC2$ are the principal component time series corresponding to the historical $EOF1$ and $EOF2$ as described above; and A, B and C are the MLR coefficients obtained for each grid point over Europe at a given level and for a given season. It can be noted that a similar methodology was first applied by Deser et al. (2004) and most recently by Deser et al. (2017), using a single leading mode of atmospheric variability and a linear regression fit to isolate the influence of internal variability on the linear trend of different variables.

The identified links between the dominant modes of Euro-Atlantic atmospheric variability and European near-surface wind speed in the present day climate are used to infer the contribution of future changes in the large-scale atmospheric

circulation to the wind speed projections in the CMIP5 RCP8.5 scenario. To do so, each GCM’s 10-day low-pass filtered 850 hPa wind over the Atlantic domain in the future simulation (\tilde{u}_{850}^{fut}) is projected onto the EOF modes obtained from the model’s historical simulation (i.e., for each individual GCM, we have verified that the EOF patterns remain unchanged between the historical and future simulations as seen in Figs. S3 and S4 of the Supplementary Material). This procedure can be described as:

$$\widehat{PCi}^{fut}(t) = EOFi^{hist}(x, y) \cdot \tilde{u}_{850}^{fut}(x, y, t) \quad (2)$$

Then, the resulting time series can be used to force the EOF-MLR model obtained from the historical simulations to derive an estimation of European wind following:

$$\widehat{ws}^{fut}(x, y, z, t) = A(x, y, z).\widehat{PC1}^{fut}(t) + B(x, y, z).\widehat{PC2}^{fut}(t) + C(x, y, z), \quad (3)$$

where A, B and C remain the same as in Eq. 1. This estimation depends exclusively on the projections of large-scale circulation change and on the present-day relationship between circulation and European windiness. Therefore, it can be anticipated that if the large-scale circulation response is not described in terms of present-day modes of variability or if the relationship between the large-scale and regional winds changes with warming, the estimated winds will differ from those projected by the models. This is not a limitation of the proposed methodology, as it will be shown that analysing these residuals is useful to suggest processes—other than the large-scale atmospheric circulation—that are important for future projections of windiness in the European region.

3 Results

3.1 Historical estimation of wind speeds

3.1.1 ERA-interim

Before examining the GCM simulations, the EOF-MLR technique is first applied to the ERA-I reanalysis to evaluate to what extent the technique is able to ‘estimate’ the observed surface wind variability over Europe.

The results from the EOF analysis applied to the cold season in ERA-I are summarized in Fig. 1. Figure 1c presents the explained variances obtained for the first 10 EOF modes and reveals that most of the variance (about 80%) can be explained by retaining the first two EOFs, which are well separated from the third EOF according to the North et al. (1982) criteria. The spatial patterns associated with these two EOFs are presented in Fig. 1a, b. To confirm that

¹ The approach adopted is therefore linear and more sophisticated schemes can clearly be constructed. However, as will be demonstrated, a linear reconstruction is sufficient for explaining a large fraction of the observed variance in surface wind speed and the linear approach is therefore justified both by its performance and intuitive simplicity.

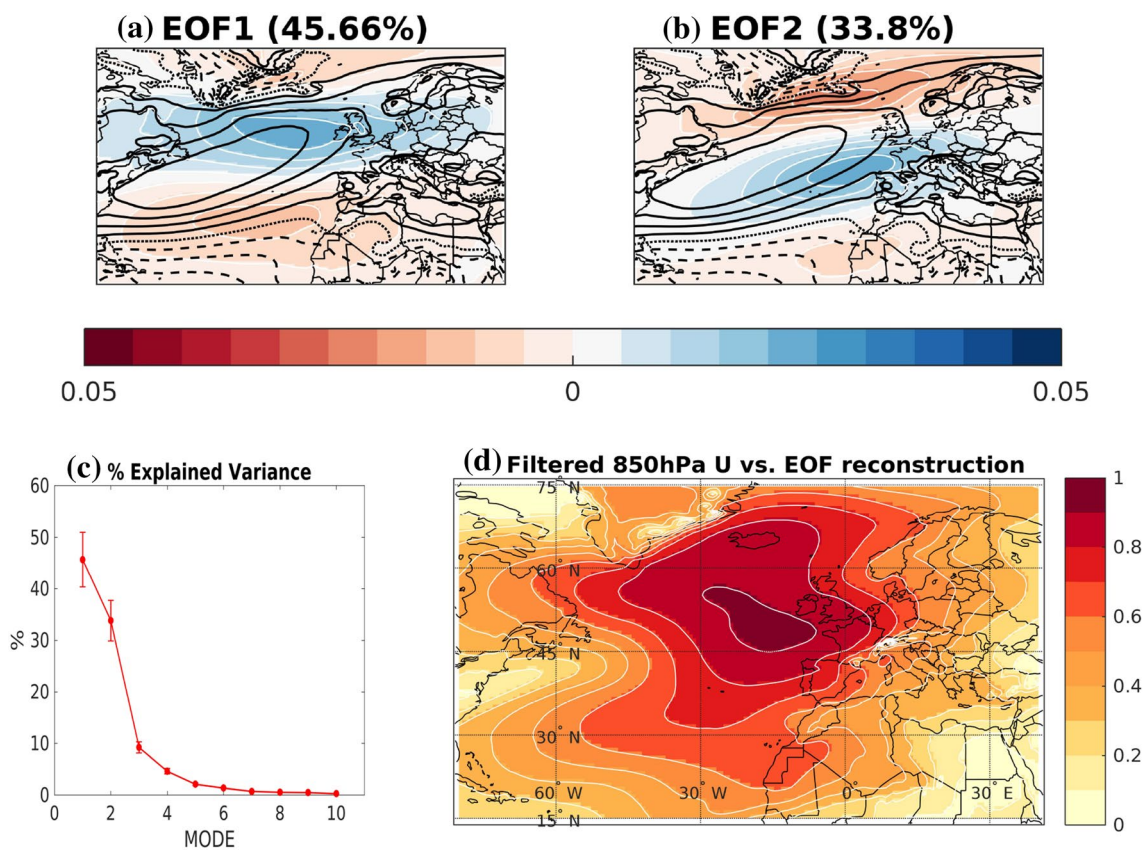


Fig. 1 EOF results for ERA-Interim cold season 10-day lowpass-filtered 850 hPa zonal wind for the period 1979–2014. **a**, **b** Present the EOF1 and 2 patterns, respectively. Black contours are 850 hPa zonal wind mean state for a qualitative comparison and are plotted every 2

m/s. Together, EOF1 and 2 explain 79.46 % of the variance. **c** presents the variance explained by the first 10 EOF patterns (in %). **d** Presents the correlation between daily 850 hPa \bar{u} wind and the EOF-MLR estimation

the first two EOFs are sufficient to represent the wind field across the whole domain, the EOFs (and corresponding PC time series) are used to estimate the 10-day low-pass filtered zonal wind values. Figure 1d shows the correlation between the estimated and original daily zonal wind, with statistically significant correlations across the North Atlantic basin, Western Europe and Northwestern Africa. The highest correlations—indicating regions where the EOF-MLR estimation is particularly good—are observed over the NE Atlantic sector, including Iceland, the United Kingdom (UK), Benelux and parts of Germany, France and the Iberian peninsula (the correlation in this region exceeds 0.8).

Figure 2 shows a similar analysis for the warm season. In this case, the first two EOF modes account for a smaller fraction of the total variance (around 68%, Fig. 2c), but are still significantly separated from the third mode. Consistently, the correlation between the EOF-MLR estimated and the daily zonal winds is therefore weaker than in winter (Fig. 2d), though the spatial pattern of the correlation is similar. Only over Southern UK and Northern France, the estimation results in correlations exceeding 0.8.

Table 2 shows that there is a link between the EOF patterns calculated here and the canonical modes of variability identified in the North Atlantic, i.e. the NAO and the EA pattern. The correlations are computed between the seasonal average of the PCs associated with EOFs 1 and 2, and the seasonal-average NAO and EA indices obtained from NOAA (see Sect. 2). Statistically significant correlations exist with the canonical patterns in both seasons, though the connection is clearly stronger in the cold season. In both cases, PC1 demonstrates a clear connection with the NAO index and PC2 with the EA index. Similar connections are found when comparing the EOFs against the canonical patterns in terms of spatial structure or by using daily-scale information (e.g., proportion of days in each phase; not shown). It is important to point out that the analysis presented here does not rely on the physical interpretation of the obtained modes of variability and, as a consequence, this does not need to be explored further. Nonetheless, we note that relating large-scale atmospheric patterns—and their representation by EOFs—to surface wind speeds is an active area of research (e.g., Brayshaw

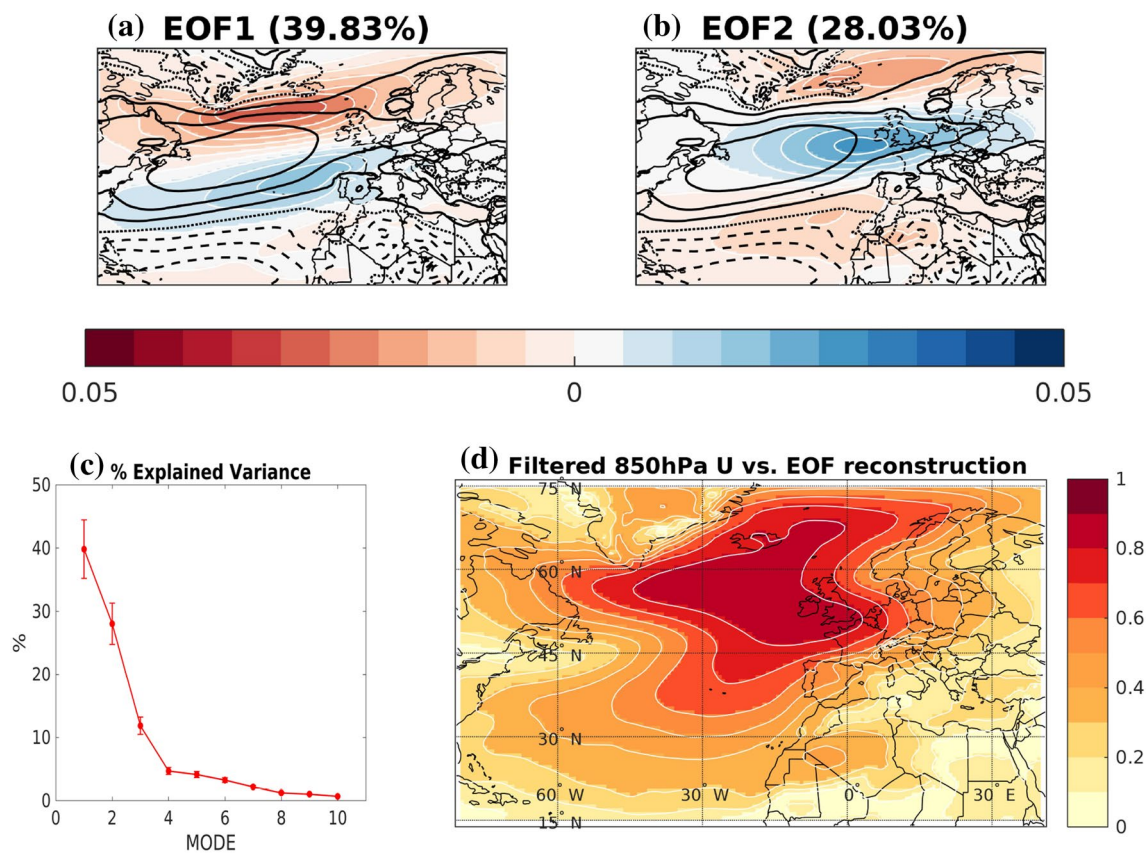


Fig. 2 Same as Fig. 1 but for the warm season. **a, b** Present the EOF1 and 2 patterns. Black contours are 850 hPa zonal wind mean state and are plotted every 2 m/s. Together, EOF1 and 2 explain 67.86 % of the variance

Table 2 Correlations between observed North Atlantic climate indices and the properties of the EOF principal components for ERA-Interim (1979–2014)

	Cold season		Warm season	
	NAO	EA	NAO	EA
PC1	0.91	-0.099	- 0.588	0.17
PC2	-0.39	0.666	0.029	0.348

Bold numbers are statistically significant at the 5% level according to a *t* test corrected for serial autocorrelations

et al. 2011; Ely et al. 2013; Hamlington et al. 2015; Zubiate et al. 2017).

The preceding analysis demonstrates that the first two EOFs—which are closely linked to the canonical NAO and EA patterns—are sufficient to capture the variability in the large-scale structure of the North Atlantic zonal wind, particularly in the cold season.

The EOF-MLR described in Sect. 2 is now applied to test the potential to estimate wind speed variability at the surface, as well as at the 850 hPa and 500 hPa levels, given the large scale flow. The coefficients of determination (R^2)

between the seasonal-average wind speed and the corresponding EOF-MLR estimations are shown in Fig. 3. The coefficients over land are in general much larger for the cold season (panels a, c and e) than for the warm season (panels b, d and f). High values (above 0.6, meaning that the EOF-MLR estimation can reproduce more than 60% of the total variance) are found for many regions of Western and Northern Europe in the cold season (e.g., Iberia reaches 0.8), but warm season correlations are relatively weak except for small regions in Northern Europe, indicating that windiness for this season is less connected to the large-scale North Atlantic zonal wind patterns. It can also be seen that, in general, the spatial patterns of R^2 are consistent with height, though the values tend to be slightly weaker at 10 m (compared to 850 hPa and 500 hPa).

It is therefore concluded that, given the North Atlantic atmospheric flow, the EOF-MLR method is capable of producing a good estimation of near-surface and lower-tropospheric wind speeds in several European regions relevant for wind energy production (e.g., Germany, France, UK, Spain) in the cold season. Given the more limited capability of the method in the warm season, the remainder of the analysis focuses solely on the cold season.

Fig. 3 Coefficient of determination R^2 for the seasonal mean wind speeds at different levels and the EOF-MLR estimates in ERA-Interim, for the cold season (left) and warm season (right). **a, b** Correspond to 500 hPa, **c, d** to 850 hPa and **e, f** to 10 m wind speeds. The black boxes on **a** indicate the definitions of focus areas

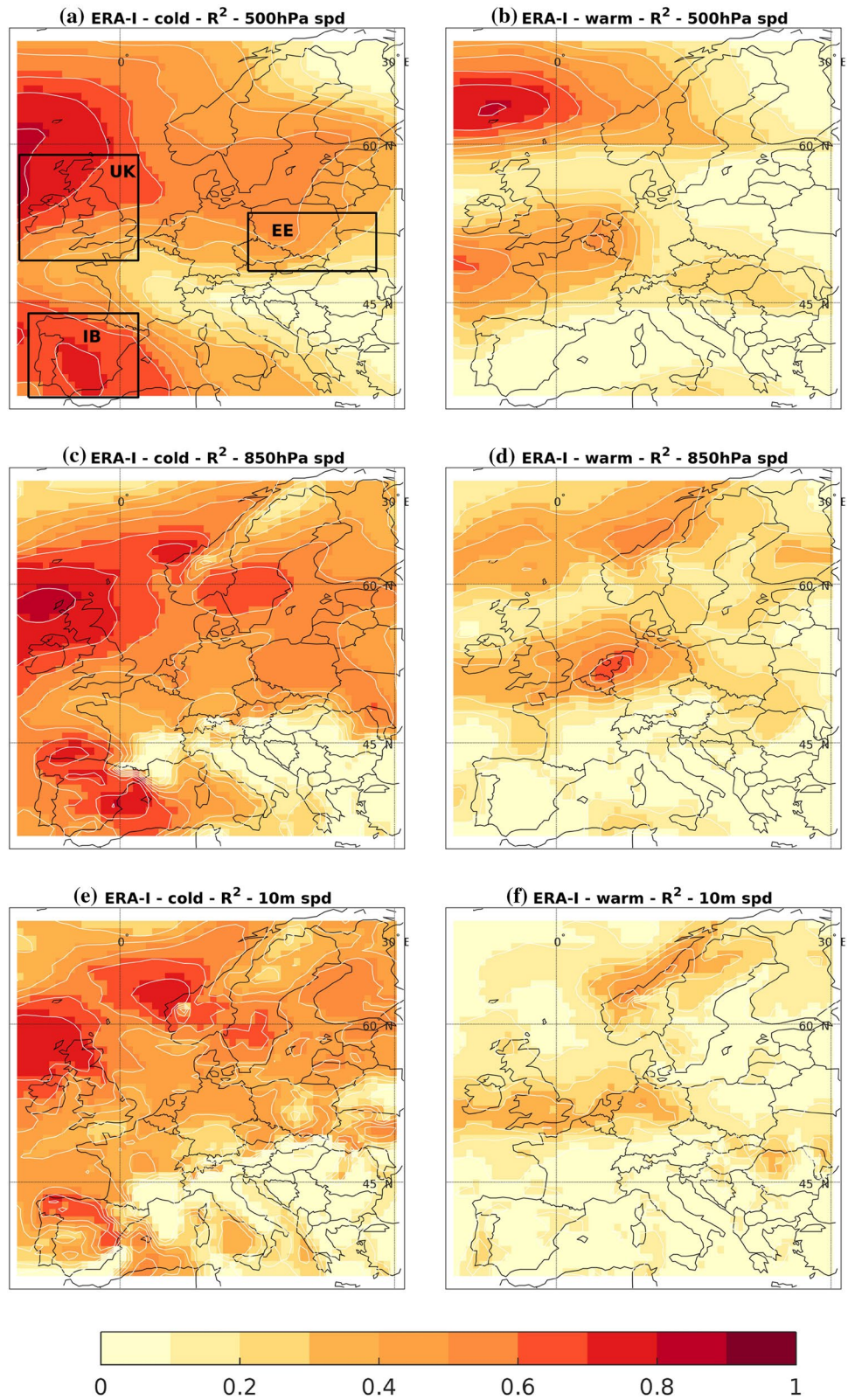
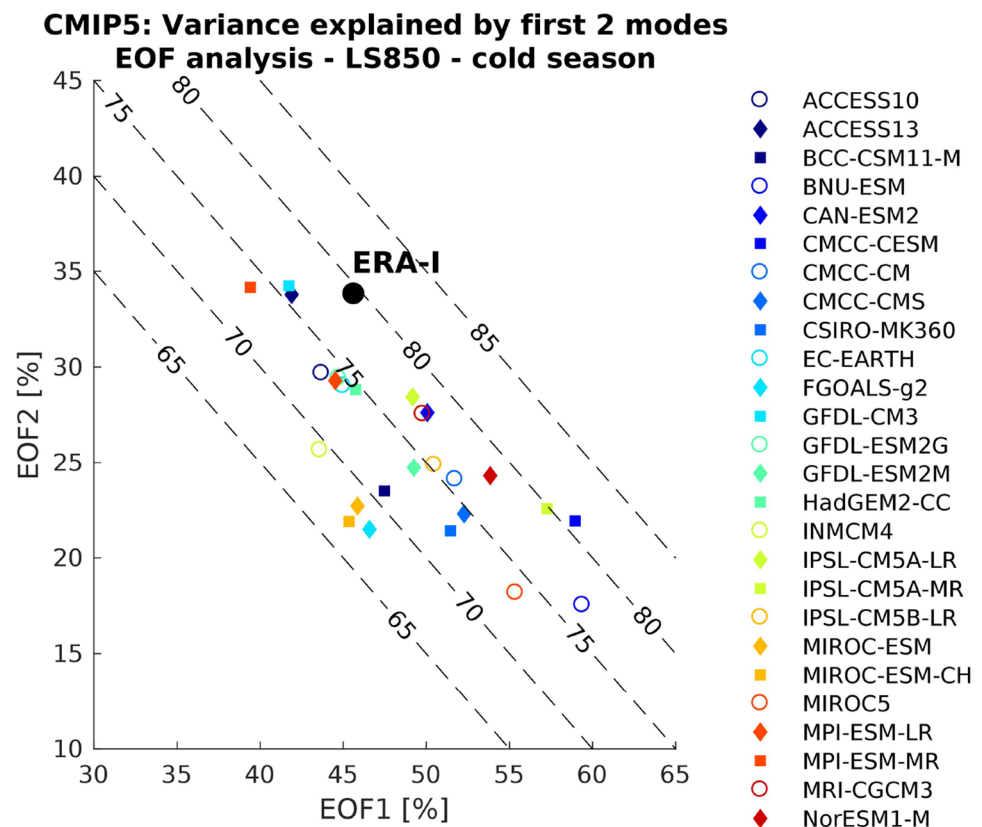


Fig. 4 Summary plot of the EOF analysis applied to the historical CMIP5 ensemble. The x axis presents the variance explained by EOF1 and the y axis for EOF2. Diagonal dashed lines correspond to different amounts of variance accumulated by the two. The black dot represents the values obtained from the ERA-I EOF analysis and individual GCMs are included as different colours and symbols



3.1.2 CMIP5

Having demonstrated that the EOF-MLR technique is able to capture the inter-annual variability of observed historical near-surface winds over Europe, a similar analysis is applied to the historical CMIP5 simulations. This enables to compare the influence that large-scale atmospheric circulation has on surface wind variations over Europe between the GCMs and reanalysis and as a result, the usefulness of the EOF-MLR estimation methodology.

The EOF-MLR technique is applied individually to the historical simulation of each GCM taken from the CMIP5 archive (i.e., for each GCM there is a unique EOF pair and MLR regression to European wind speed). The EOF patterns obtained for each model are included in the Supplementary Material (Figs. S1 and S2).

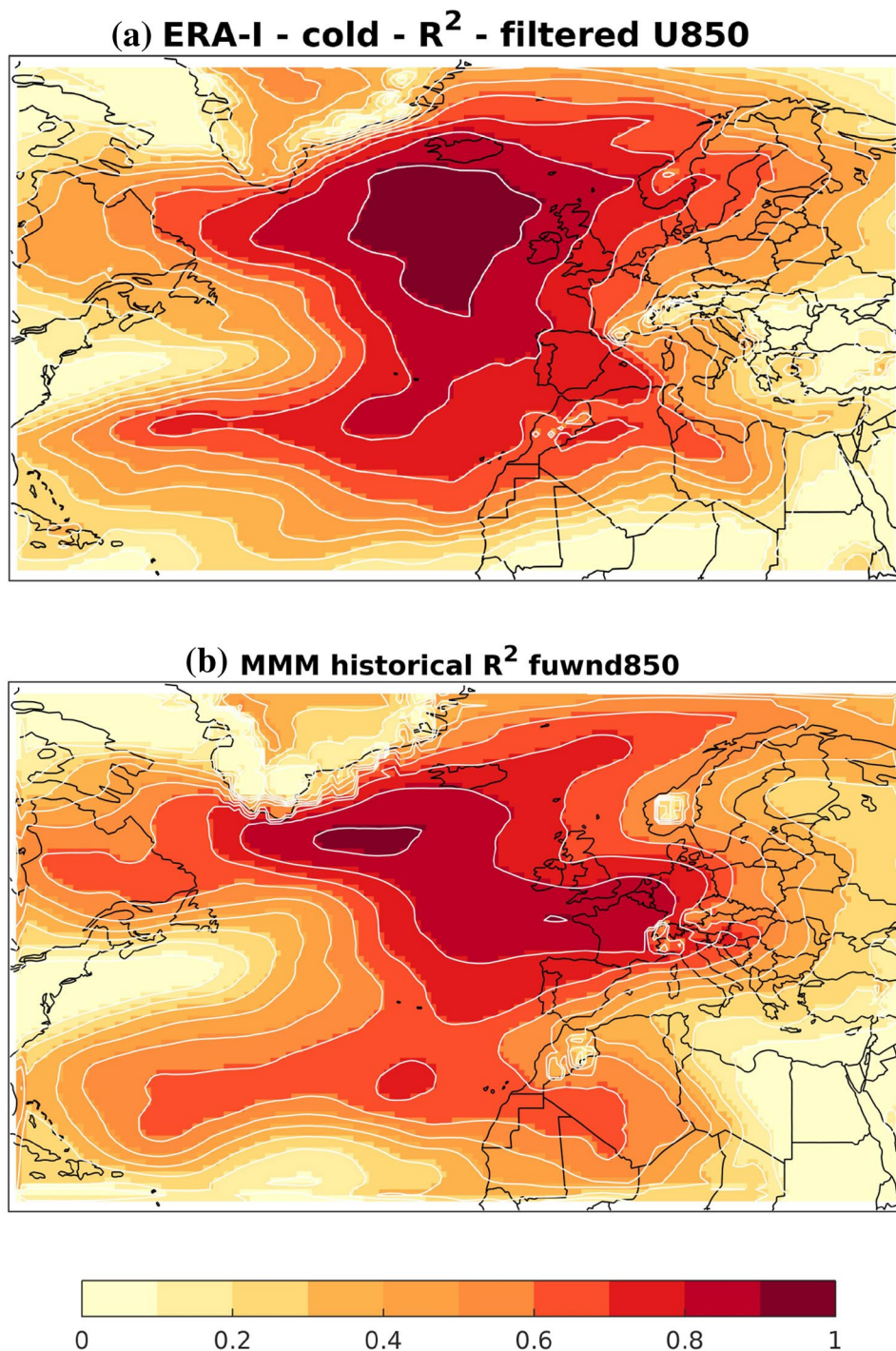
Figure 4 summarises the EOF analysis. It is noted that all but two GCMs underestimate the total variance accounted by the first two EOF patterns. At the same time, most GCMs overestimate the variance explained by EOF1 and underestimate that explained by EOF2. The limitations of the representation of the leading patterns of North Atlantic atmospheric variability in CMIP5 models has already been discussed by other authors (e.g., Davini and Cagnazzo 2014) and are therefore not further investigated here.

As in Sect. 3.1.1, the PC time series corresponding to EOFs 1 and 2 are linked to the near-surface wind speeds using a MLR, and the resulting EOF-MLR are used to estimate time series of near-surface wind speeds over Europe.

Figure 5 shows the ability of the EOF-MLR method to estimate 10-day low-pass filtered 850 hPa zonal wind in the North Atlantic domain. The spatial structure of the coefficient of determination between the original and estimated zonal wind fields for ERA-Interim (Fig. 5a), as well as the CMIP5 historical simulations MMM (Fig. 5b), are qualitatively similar with strongest values offshore and in Western Europe. In addition, it can be seen that the estimate is consistent in strength and spatial pattern with reanalysis, though with relatively lower values over the UK area and relatively higher values penetrating inland along France.

The seasonal averages of the European wind speed time series from each GCM are compared with the respective EOF-MLR estimations on a region-by-region basis (for the boxes indicated in Fig. 3), and the results are summarised for two vertical levels in three regions in Fig. 6. For both levels, observed coefficients of determination are high and significant for the UK and Iberia (IB) boxes (assessed through an F-test at the 5% level), indicating that the EOF-MLR method is able to produce a good estimation of the inter-annual variability of cold season wind speed simulated by each GCM over these areas (i.e., within each GCM the large-scale

Fig. 5 Cold season coefficients of determination (R^2) between 10-day filtered 850 hPa zonal wind over the North Atlantic sector and the EOF-MLR estimated fields. **a** Corresponds to ERA-I and **b** to the CMIP5 multi-model mean (MMM) considering only the 20-model subset providing data at all levels



atmospheric circulation associated with EOFs 1 and 2 is strongly connected to surface wind speed anomalies at seasonal time scales). For the UK box (Fig. 6a and d), the coefficients between GCM-based and estimated seasonal average wind speeds are also generally comparable in magnitude to the historical correlations seen in ERA-I (the MMM value for 10 m is almost identical to the one obtained from ERA-I), though some models slightly over- or underestimate the

strength of the connection. For IB, a strong link between the large-scale atmospheric circulation and near-surface wind remains but is generally weaker than in ERA-I and than the coefficients seen for UK in the GCMs, particularly at the 10 m level (Fig. 6b). In the case of the Eastern Europe (EE) box, the observed correlations are much weaker (slightly above 0.4 for 500 hPa) and most models noticeably underestimate the strength of the connection, especially at 10 m.

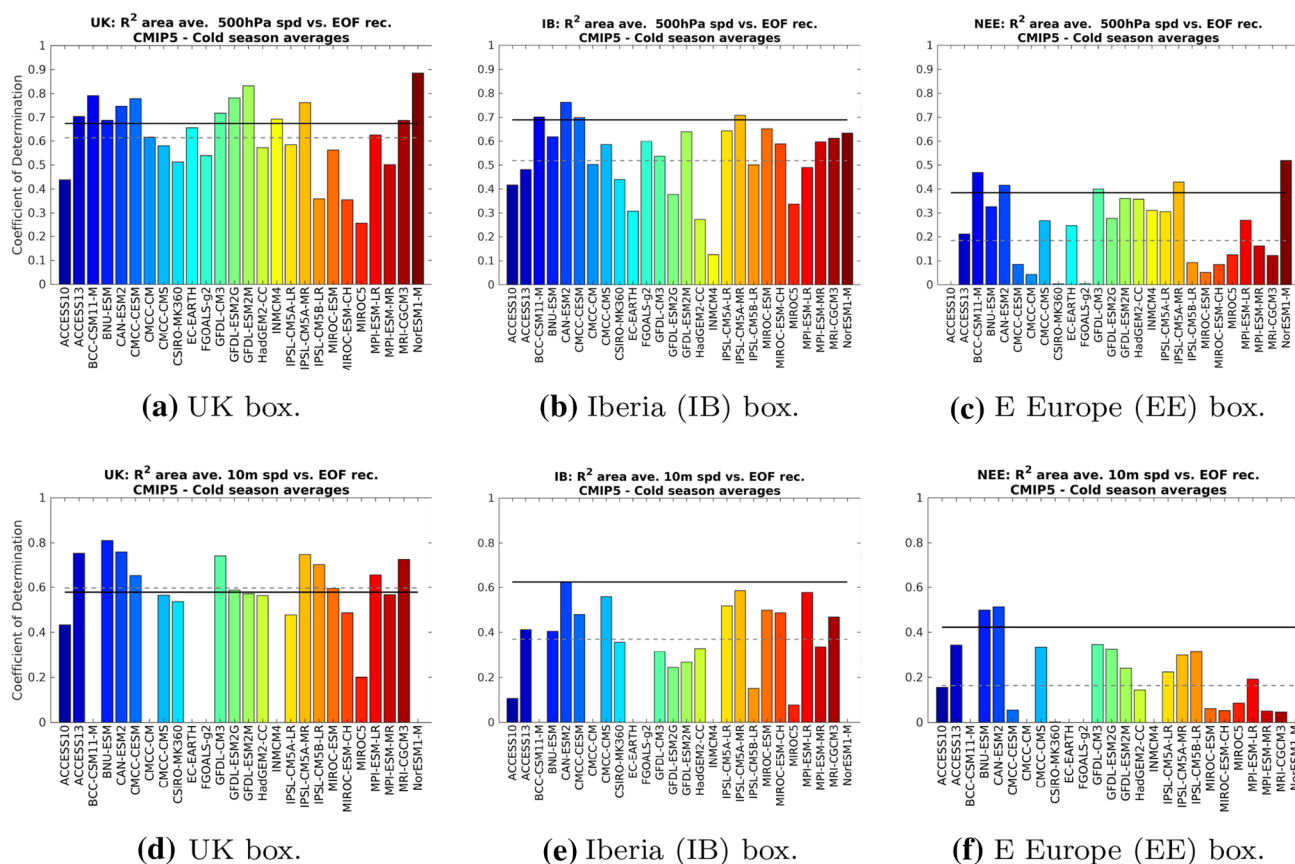


Fig. 6 Coefficients of determination between seasonal mean wind speed at two levels and the corresponding EOF-MLR estimates. **a–c** Correspond to 500 hPa speeds and **d–f** correspond to 10 m speeds.

The grey dashed horizontal line presents the multi-model mean value, and the black continuous horizontal line presents the value obtained from ERA-Interim

These results suggests that, as in the case of ERA-I, the EOF-MLR estimation is capable of capturing the main sources of variability in seasonal wind speeds over Europe and the link between historical North Atlantic variability and windiness over Western Europe. Over Central and Eastern Europe the connection between wind speed and the large-scale atmospheric circulation is weaker. In both cases, however, the GCMs have a tendency to underestimate the influence of the large-scale atmospheric circulation on European wind speeds, particularly at near-surface levels (10 m rather than 500 hPa). The coefficients of determination fields for the estimates of wind speed at each level and for each model are available in the Supplementary Material (S5, S6, S7 and S8).

3.2 Estimation of future wind speeds

The EOF-MLR technique described in Eq. 3 was then applied to the RCP8.5 CMIP5 runs. As described in Sect. 2.1, the EOF patterns and MLR parameters obtained from the CMIP5 historical simulations were used to estimate the European near-surface wind speed projected changes

associated with the response of the North Atlantic large-scale atmospheric circulation to climate change.

Figure 7 shows the multi-model mean R^2 results obtained by applying the EOF-MLR model to the CMIP5 historical and future simulations. For each of the three levels the MMM shows qualitatively similar coefficients of determination (and thus explained variances) in the future simulations and in the historical simulations. Indeed, the coefficient is higher in many regions, which suggests that a larger fraction of regional wind variability is connected to the North Atlantic large-scale atmospheric circulation in the future climate compared to the present day.

3.3 Projected changes

The preceding analysis demonstrates that the EOF-MLR technique is able to represent the impact of variations in large-scale North Atlantic atmospheric circulation variability on western European wind speeds, both for the historical and future CMIP5 simulations. This section now uses the same methodology to assess the contribution of projected future changes in the large-scale North Atlantic atmospheric

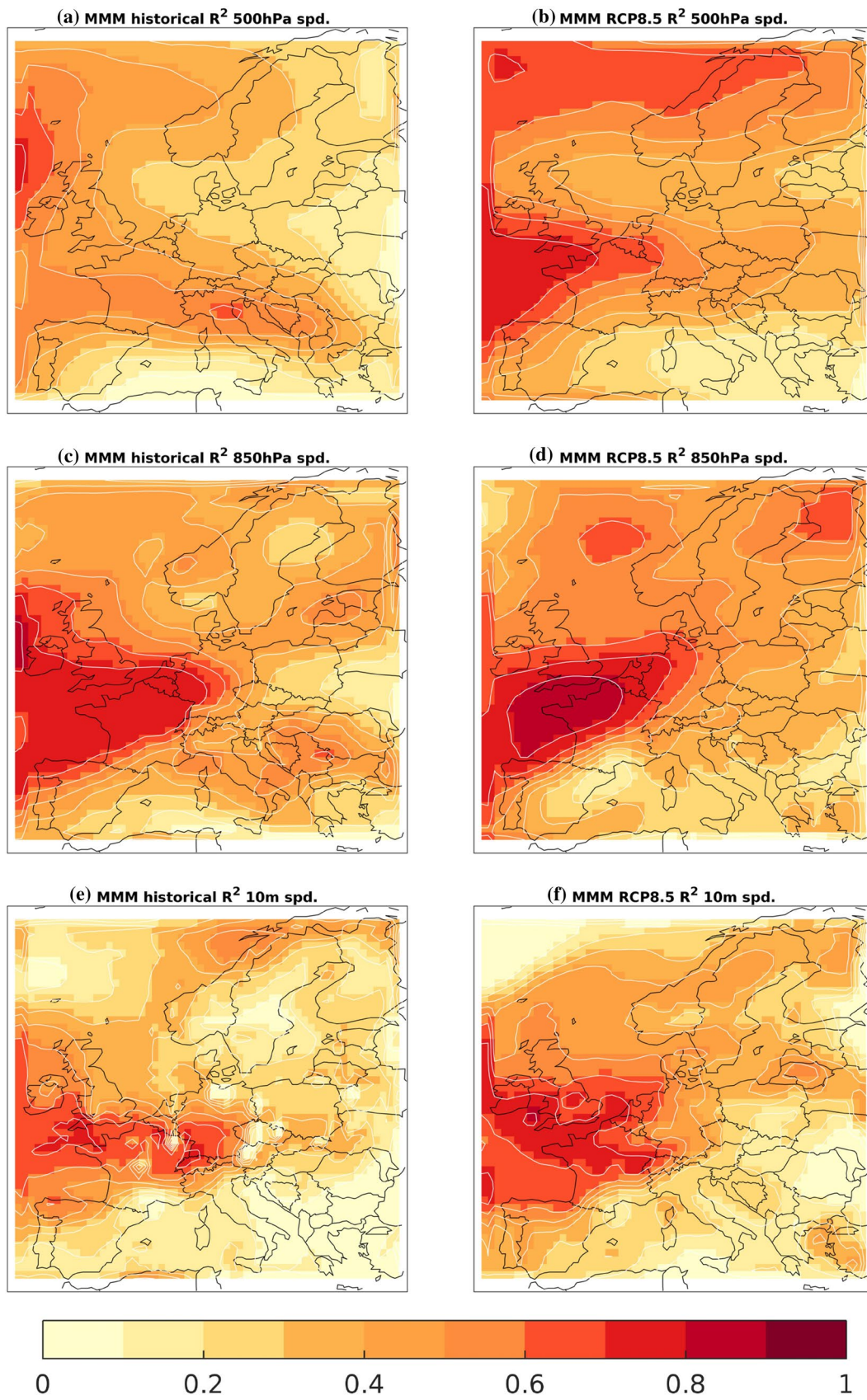
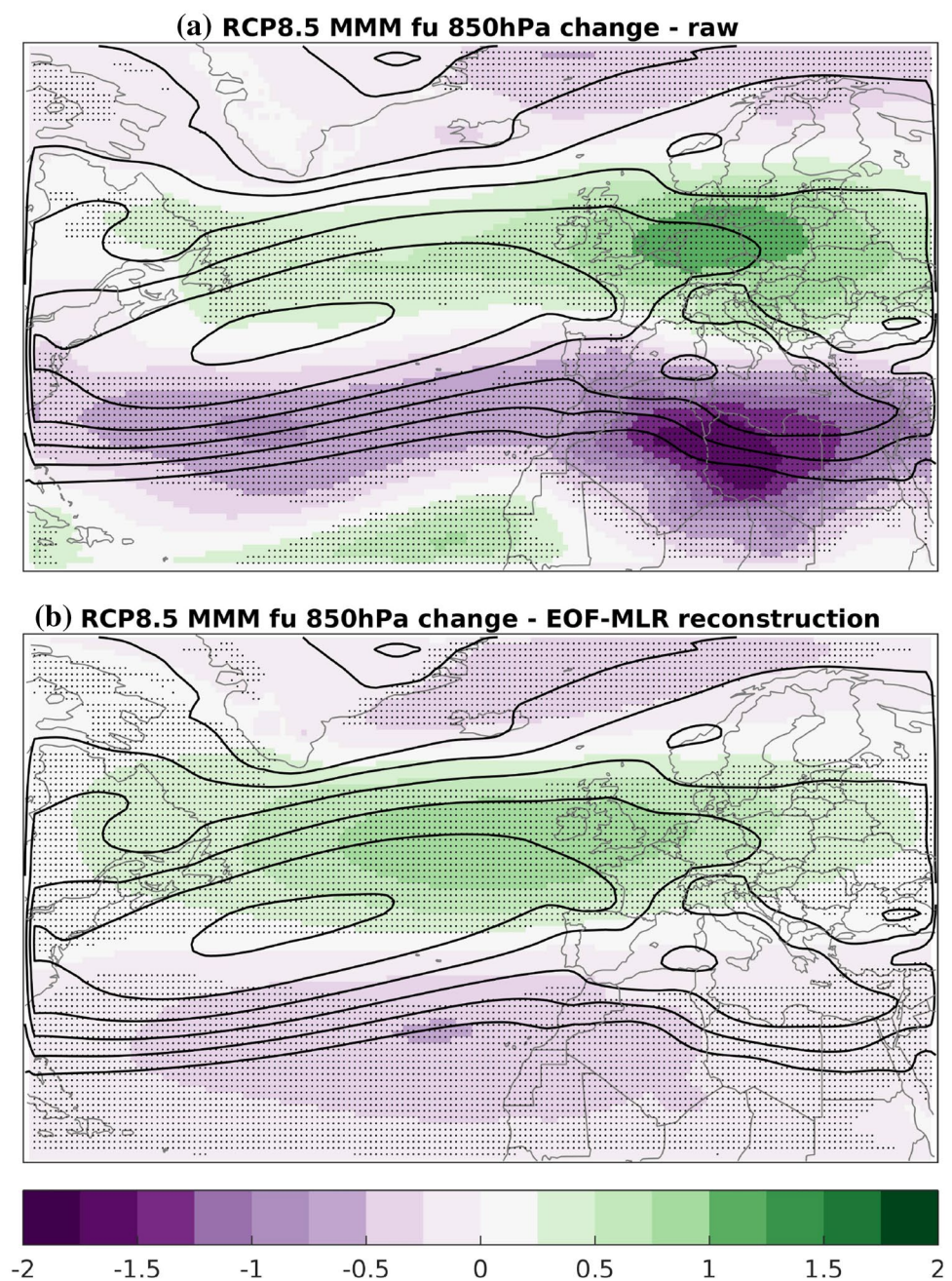


Fig. 7 Multi-model mean cold season coefficients of determination (R^2) between wind speed and the EOF-MLR estimated fields at 500 hPa (a, b), 850 hPa (c, d) and 10 m (e, f), for the historical (left) and RCP8.5 (right) runs

Fig. 8 Multi-model mean (MMM) GCM-based change for the 10-day filtered 850 hPa zonal wind field (a) and the EOF-MLR estimated fields (b) in m/s. The black contours represent the historical MMM mean field plotted every 2 m/s. The small black dots indicate regions where at least 70% of the models agree on the sign of the change



circulation to changes in European near-surface wind climate. The near-surface wind speed changes estimated from the EOF-MLR method are therefore contrasted with the wind speed changes projected by each individual GCM.

Figure 8 compares the multi-model mean (MMM) seasonal mean response (i.e. future–historical) in the filtered zonal wind at 850 hPa projected by the models (a) and that estimated by the EOF-MLR method (b). As found in previous studies (e.g., Simpson et al. 2014; Zappa et al. 2015b), the MMM response is consistent with a poleward shift of the North Atlantic jet, with a westerly enhancement in Central and Northern Europe, and weaker westerlies over most

of Iberia and the Southern North Atlantic. The EOF-MLR method successfully captures this poleward shift, but the response in the estimated zonal wind speed pattern peaks over the ocean on the Eastern edge of the basin, rather than in Europe. In particular, the EOF-MLR method underestimates the westerly response in Central Europe and the easterly response in North Africa. These features are associated with an anticyclonic circulation response over the Mediterranean, which despite being robust across the models does not appear to project onto the historical leading patterns of variability (e.g., Zappa et al. (2015a) and references therein). As such, these features are not captured by the EOF-MLR

estimation method. It is therefore important to emphasise that while the EOF-MLR method appears to provide a good representation of change in the North Atlantic plus Northern and Western Europe, it can only do so because the climate change pattern projects strongly onto the existing patterns of historical variability.

Thus, although the variability in the future zonal wind climate over the Mediterranean is well represented by the EOF-MLR, the climate change signal is not. The subsequent analysis is therefore primarily focused over Western Europe (in particular the UK and Iberia boxes), where the EOF-MLR is better at capturing the large-scale response in the atmospheric circulation.

The MMM and EOF-MLR estimated changes in near-surface wind over Europe are shown in Fig. 9 (note that the values are normalised by the GCM-based historical mean speed on each level for ease of comparison). For the higher vertical levels (500 hPa and 850 hPa; a–d) the EOF-MLR estimation of the projected change (right panels) shows a similar pattern to the GCM-based wind speed projections, with increases over the UK and France reaching zonally into the continent (between 2 and 4% of the historical wind speed mean). However, the eastward penetration of the increased wind speeds is less pronounced for the estimation than the GCM data would suggest, particularly at 500 hPa, decaying rapidly over Germany and Poland. This is consistent with the previously identified limitation of the EOF-MLR method: the circulation response over the Mediterranean does not project onto the dominant modes of internal atmospheric variability.

Consistently with the upper levels, the EOF-MLR method also estimates a future increase in 10 m wind speeds over Central/Western Europe of up to 4% of the historical mean (Fig. 9f). However, this is not generally found in the GCM-based projections (Fig. 9e). In particular, over most land areas, models project a future weakening (rather than an increase) in surface wind speeds, with the exception of small regions over France, Southern Scandinavia and Northern Germany. Furthermore, this projected weakening of 10 m wind speeds is strikingly different from the projected wind speed increase found for 850 hPa (Fig. 9c). The strong vertical structure in the wind speed response and the inability of the EOF-MLR method to capture the sign of the response at the surface suggest that boundary layer processes are playing a key role in the GCM-based near-surface wind speed projections.

Figures 10 and 11 put the focus on the UK and IB boxes. These are regions which are both important players in European wind-energy production, and areas where the EOF-MLR methodology was demonstrated to produce a good estimation of both future variability (at all vertical levels) and change (at 850 hPa and 500 hPa). For each level, these figures contain a scatter plot comparing the GCM-based and the EOF-MLR

estimated changes, and a bottom panel presenting the residuals: i.e., the difference between the GCM and the EOF-MLR reconstruction.

For the UK box, the GCM-based changes for 10 m show significant spread across the CMIP5 ensemble, with little agreement in the sign of change leading to very small changes projected in the MMM (Fig. 10a, less than a 0.5% decrease with respect to the historical mean). At higher levels (850 and 500 hPa) the signal remains mixed, though an overall tendency towards a positive change emerges. By contrast, the EOF-MLR estimated changes show an increase in wind speed in almost every GCM and at all levels (consistent with the patterns shown in Fig. 9). The residuals are predominantly negative and consistent in sign across the three vertical levels, though the magnitude of the MMM residual decreases with height. Overall, this suggests that the change in large-scale atmospheric circulation would drive an increase in UK near-surface wind speeds (at 10 m, of around 2% of the historical mean), but this is somewhat compensated by a decrease associated with processes that cannot be directly linked to the modes of large-scale North Atlantic atmospheric variability. The magnitude of the mean residual term decreases with height (Fig. 10d, f), further suggesting that this residual may be associated with boundary-layer or surface processes.

For the Iberian box (Fig. 11) the reasoning is similar, though the implications for near-surface wind climate are markedly different. In the GCM-based projections, both 10 m and 850 hPa show a strong decrease in wind speed in almost all GCMs, while there is little consensus between the GCM projections at 500 hPa. The EOF-MLR estimated wind speed projection, however, qualitatively resembles the 500 hPa change with wide spread between models and very weak change in the MMM. The reduction in wind speeds at 10 m and 850 hPa therefore lies solely in the residual term (which is again negative, as in the UK box).

Another important point that arises from these scatter plots is the fact that the inter-model spread remains large in the EOF-MLR estimation, suggesting that the uncertainty in the GCM projections for the UK and Iberia can be explained to a large extent by differences in the response to North Atlantic atmospheric variability.

This analysis therefore seems to strongly suggest that GCM-derived near-surface wind projections over Europe (particularly Western Europe) arise as the joint effect of multiple processes, rather than being simply a response to North Atlantic large-scale atmospheric circulation changes.

4 Summary and discussion

This study explores the connection between near-surface wind projections over Europe and changes in the large-scale atmospheric circulation over the Atlantic-European sector.

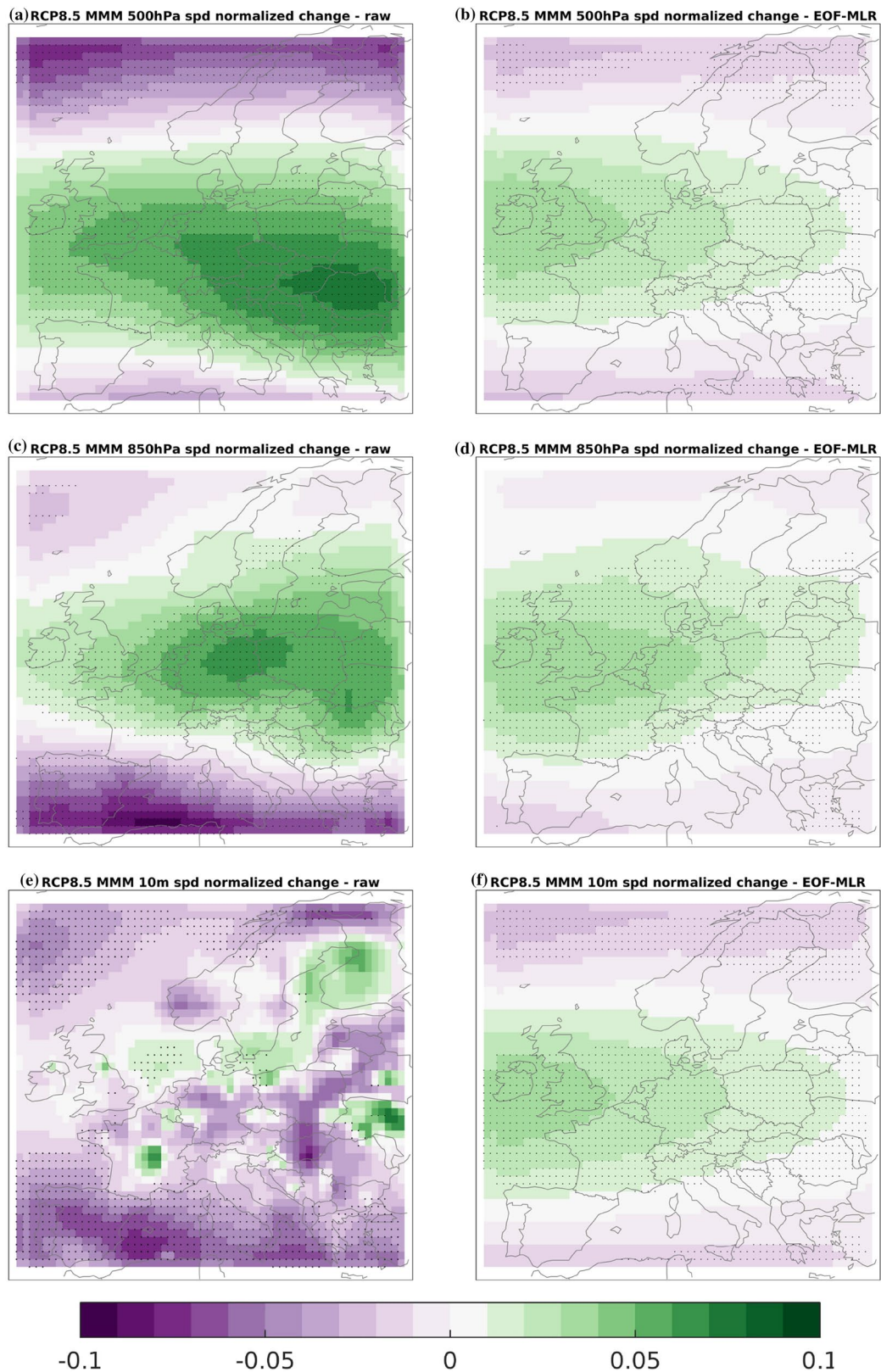


Fig. 9 Multi-model mean (MMM) normalised changes in wind speed between the RCP8.5 and historical periods obtained from the GCM-based (left) and EOF-MLR estimated (right) fields. In every case, the wind speed difference between the two periods was normalised by the

average historical wind speed of the specific level. **a, b** correspond to 500 hPa, **c** and **d** to 850 hPa, and **e, f** to 10 m. Black dots indicate regions where at least 70% of the models agree on the sign of the change

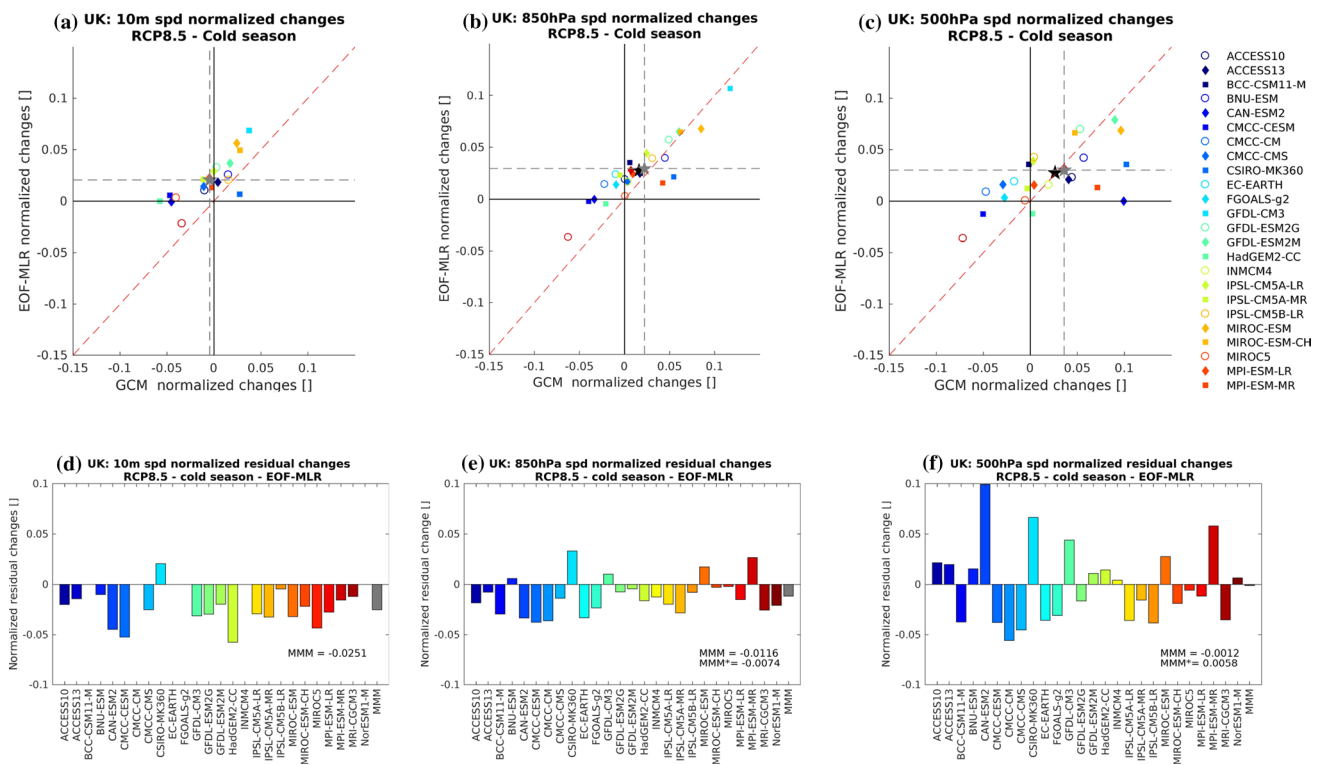


Fig. 10 UK regional normalised changes in 10 m (a, d), 850 hPa (b, e) and 500 hPa (c, f) speeds. **a–c** The scatter plots compare the GCM and EOF-MLR projections of the wind speed change for the UK box. The grey star, which is also indicated by the grey dashed cross-lines, corresponds to the multi-model mean (MMM) obtained from the set

of common models. **d–f** The residuals (difference between GCM-based and EOF-MLR projections) are shown on the bottom row. All the presented responses and residuals are normalised by the average historical speed of the corresponding level. The MMM* value corresponds to the ensemble mean of models available in all levels

It is demonstrated that GCM projections of surface wind speed change during the 21st century cannot be explained as a result of changes in existing modes of large-scale atmospheric circulation alone (broadly corresponding to the NAO/EA patterns and North Atlantic jet).

A statistical method employing EOFs and a multiple linear regression model (EOF-MLR) is applied to both observational (ERA-Interim) and CMIP5 historical GCM simulations to isolate the European wind speed signals associated with changes in the large-scale atmospheric circulation over the North Atlantic. The connection between the large-scale circulation and surface wind speeds was found to be stronger in the cold season (NDJFMA) than the warm season (MJJASO) in ERA-Interim. In both seasons, the link is strongest over the Atlantic, decaying eastward into the European continent, though strong connections exist for Western Europe, including Ireland, UK, France, Germany, southwestern Scandinavia and Iberia, particularly in the cold season.

The EOF-MLR was subsequently applied to estimate the future changes in European wind speed associated with projected changes in large-scale atmospheric circulation for the 21st century. In the free troposphere, the estimated

wind speed changes are consistent with the GCM projections across much of Western and Northern Europe: i.e., the change in wind speed estimated by the EOF-MLR method is similar to the change in the raw GCM near-surface wind. However, near the surface, the EOF-MLR estimation reveals a substantially different pattern of changes over Europe when compared to the equivalent raw GCM near-surface wind, implying that the GCMs near-surface wind speed changes cannot be attributed to changes in large-scale atmospheric circulation alone. For the UK, the estimated large-scale component suggests a moderate increase in wind speed under RCP8.5 in the MMM (compared to no change in the GCM-based MMM projections) whereas for Iberia the estimated large-scale circulation change suggests no change in near-surface wind speeds (compared to a negative change in the GCM-based MMM near-surface wind speed projections). The difference between the GCM-based and estimated changes therefore reveals a negative 'residual' in both cases—likely associated with changes in boundary layer processes under climate change, though further investigations would be necessary to confirm the causes and to compare to more recent developments in the representation of PBL processes (e.g., Shin et al. 2018; Gross et al. 2018). It is also noteworthy

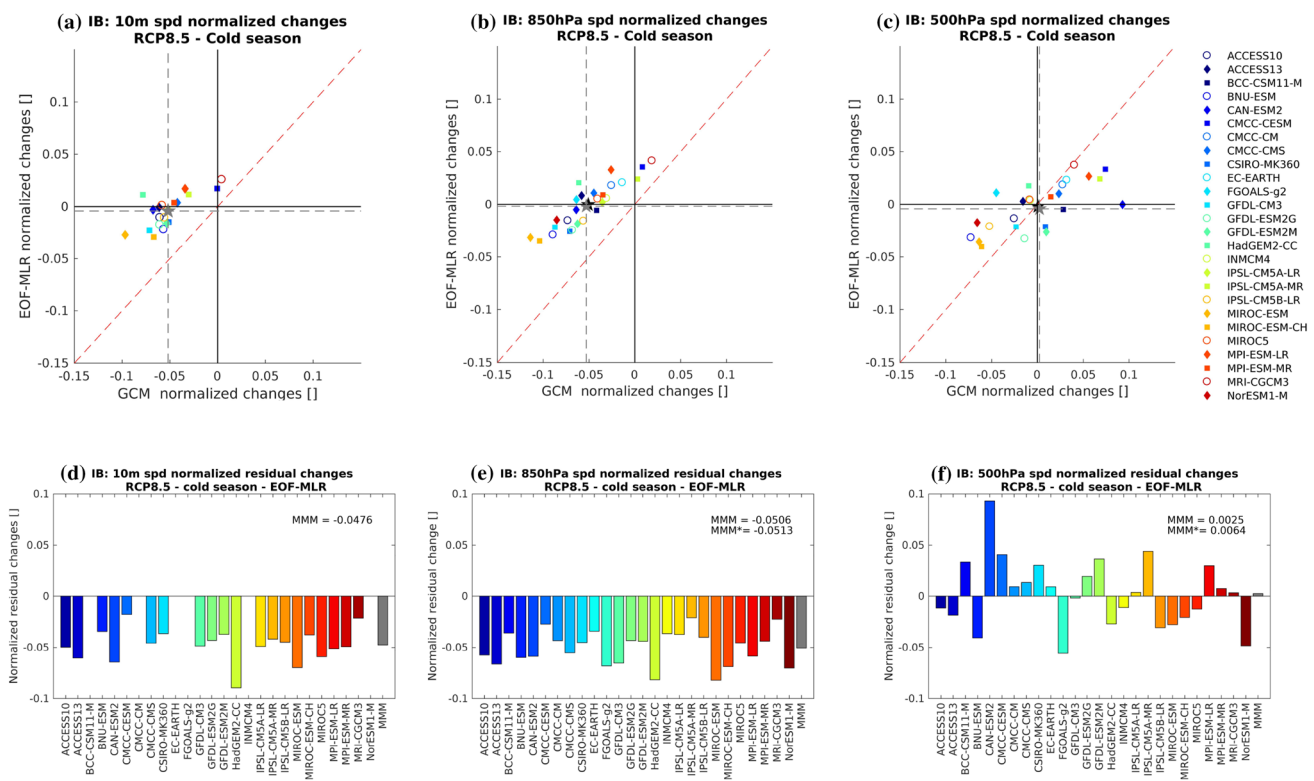


Fig. 11 Same as Fig. 10 but for the Iberia (IB) box

that this residual is even more negative over the surrounding ocean areas, suggesting that the potential implications for off-shore wind power generation may be greater.

The use of the EOF-MLR methodology proved adequate to isolate the influence of the large-scale atmospheric variability on climate projections of near-surface winds over much of Europe. Two key lessons are drawn from this analysis. Firstly, it has been shown that, in general, GCMs have deficiencies capturing the link between North Atlantic large-scale circulation and near-surface windiness. In terms of directly projecting future near-surface wind speed changes from GCMs, the quality of their simulation of the link between the large-scale circulation and near-surface wind variability (on timescale of days to months) may therefore offer a useful metric for selecting or weighting an ensemble of GCM projections. An interesting question for further research is the extent to which this weak bias in the strength of this link can be rectified by regional climate models (RCMs) downscaling (as seen in, e.g., EURO-CORDEX or climate impacts simulations such as UKCP18 <https://www.metoffice.gov.uk/research/collaboration/ukcp>, EUCP <https://www.eucp-project.eu>).

Secondly, it is clear that much of the spread in future near-surface wind speed projections from GCMs arises from differences in their large-scale circulation responses (the residual is remarkably consistent across different

GCMs). This suggests that the quality and coherence of climate change projections of surface wind speed are strongly influenced by the wider projections of large-scale atmospheric circulation. In terms of RCM downscaling studies of wind-speed projections (such as Tobin et al. 2016), this suggests that the selection of parent GCM simulations which are used to drive the RCM downscaling is very important. In particular, if the parent GCMs fail to adequately sample potential future large-scale circulation changes, then a biased near-surface wind speed projection may result. Conversely, taking a multi-model mean over a number of climate projections sampling a range of future large-scale circulation states (associated with a mixture of positive and negative near-surface wind speed changes), could lead to cancellation: the multi-model mean may therefore tend to underestimate the extent to which changes in near-surface wind climate are possible. “Storyline” approaches for future near-surface winds may offer a novel approach to deal with this deep uncertainty (e.g., Zappa and Shepherd 2017).

This work has been the first one to attempt to link near-surface wind speed changes over Europe with changes in North Atlantic large-scale variability. By doing so, it has shown that wind speed changes projected by CMIP5 GCMs for the upper levels are consistently connected to such processes but that that is not the case for surface wind speeds.

Ultimately, the analysis presented suggests that CMIP5 GCM-based wind speed projections over Europe represent the sum of two potentially opposing processes—neither of which is necessarily well characterised by the current generation of GCMs in CMIP5. The first process is the well-studied problem of changes in the large-scale atmospheric circulation, around which many uncertainties remain as discussed in the Introduction. The second process, however, is likely associated with changes in the surface boundary layer. Given the widespread interest in surface wind climate—not least in support of the expansion of renewable energies—it is therefore vital that the boundary layer is well-represented in GCMs and changes in its structure (associated with both interannual climate variability and long term change) are well understood. Recent studies have shown a clear connection between boundary-layer schemes and parameterizations in the GCMs and the representation of near-surface wind and circulation features (e.g., Lindvall et al. 2017; Gross et al. 2018; Shin et al. 2018). Indeed, given the difficulties in confidently simulating changes in large-scale atmospheric circulation, it may be possible to make more rapid progress in understanding this boundary-layer component than in the large-scale. Until such understanding is developed, however, projections of future near-surface wind climates may be best viewed with some caution.

Acknowledgements PG and DB were supported by the PRIMAVERA project, funded by the European Union's Horizon 2020 programme, Grant Agreement no. 641727. GZ was supported by the ACRCC project (ERC advanced Grant 339390). We wish to thank two anonymous reviewers for their comments on an earlier version of the manuscript.

Open Access This article is distributed under the terms of the Creative Commons Attribution 4.0 International License (<http://creativecommons.org/licenses/by/4.0/>), which permits unrestricted use, distribution, and reproduction in any medium, provided you give appropriate credit to the original author(s) and the source, provide a link to the Creative Commons license, and indicate if changes were made.

References

- Arora VK, Scinocca JF, Boer GJ, Christian JR, Denman KL, Flato GM, Kharin VV, Lee WG, Merryfield WJ (2011) Carbon emission limits required to satisfy future representative concentration pathways of greenhouse gases. *Geophys Res Lett*. <https://doi.org/10.1029/2010GL046270>
- Barnston AG, Livezey RE (1987) Classification, seasonality and persistence of low-frequency atmospheric circulation patterns. *Mon Weather Rev* 115(6):1083–1126. [https://doi.org/10.1175/1520-0493\(1987\)115<1083:CSAPOL>2.0.CO;2](https://doi.org/10.1175/1520-0493(1987)115<1083:CSAPOL>2.0.CO;2)
- Bentsen M, Bethke I, Debernard JB, Iversen T, Kirkevåg A, Seland Ø, Drange H, Roelandt C, Seierstad IA, Hoose C, Kristjánsson JE (2013) The norwegian earth system model, NorESM1-M—Part 1: Description and basic evaluation of the physical climate. *Geoscientific Model Dev* 6(3):687–720. <https://doi.org/10.5194/gmd-6-687-2013>

- Bichet A, Wild M, Folini D, Schr C (2012) Causes for decadal variations of wind speed over land: sensitivity studies with a global climate model. *Geophys Res Lett* 39(11):111701. <https://doi.org/10.1029/2012GL051685>
- Bloomfield HC, Brayshaw DJ, Shaffrey LC, Coker PJ, Thornton HE (2016) Quantifying the increasing sensitivity of power systems to climate variability. *Environ Res Lett* 11(12):124025. <http://stacks.iop.org/1748-9326/11/i=12/a=124025>
- Blumenthal MB, Bell M, del Corral J, Cousin R, Khomyakov I (2014) Iri data library: enhancing accessibility of climate knowledge. *Earth Perspect* 1(1):19. <https://doi.org/10.1186/2194-6434-1-19>
- Brayshaw DJ, Troccoli A, Fordham R, Methven J (2011) The impact of large scale atmospheric circulation patterns on wind power generation and its potential predictability: A case study over the UK. *Renew Energy* 36(8):2087–2096. <https://doi.org/10.1016/j.renene.2011.01.025>
- Carvalho D, Rocha A, Gmez-Gesteira M, Santos CS (2017) Potential impacts of climate change on European wind energy resource under the cmip5 future climate projections. *Renew Energy* 101:29–40. <https://doi.org/10.1016/j.renene.2016.08.036>
- Collier M, Uhe P (2012) CMIP5 datasets from the ACCESS1.0 and ACCESS1.3 coupled climate models. CAWCR, CSIRO/BOM, Australia. https://www.cawcr.gov.au/technical-reports/CTR_059.pdf
- Collier M, Jeffrey S, Rotstain L, Wong K, Dravitzki S, Moeseneder C, Hamalainen C, Syktus J (2011) The CSIRO-Mk3-6-0 Atmosphere-Ocean GCM: participation in CMIP5 and data publication. In: MODSIM11 international congress on modelling and simulation. <https://www.mssanz.org.au/modsim2011/F5/collier.pdf>
- Collins WJ, Bellouin N, Doutriaux-Boucher M, Gedney N, Halloran P, Hinton T, Hughes J, Jones CD, Joshi M, Liddicoat S, Martin G, O'Connor F, Rae J, Senior C, Storch S, Totterdell I, Wiltshire A, Woodward S (2011) Development and evaluation of an Earth-System model—HadGEM2. *Geoscientific Model Dev* 4(4):1051–1075. <https://doi.org/10.5194/gmd-4-1051-2011>
- Davini P, Cagnazzo C (2014) On the misinterpretation of the north atlantic oscillation in CMIP5 models. *Clim Dyn* 43(5):1497–1511. <https://doi.org/10.1007/s00382-013-1970-y>
- Dee DP, Uppala SM, Simmons AJ, Berrisford P, Poli P, Kobayashi S, Andrae U, Balmaseda MA, Balsamo G, Bauer P, Bechtold P, Beljaars ACM, van de Berg L, Bidlot J, Bormann N, Delsol C, Dragani R, Fuentes M, Geer AJ, Haimberger L, Healy SB, Hersbach H, Hólm EV, Isaksen I, Kållberg P, Köhler M, Matricardi M, McNally AP, Monge-Sanz BM, Morcrette J-J, Park B-K, Peubey C, de Rosnay P, Tavolato C, Thépaut J-N, Vitart F (2011) The ERA-interim reanalysis: configuration and performance of the data assimilation system. *Q J R Meteorol Soc* 137(656):553–597. <https://doi.org/10.1002/qj.828>
- Deser C, Magnussdottir G, Saravanan R, Phillips A (2004) The effects of north atlantic sst and sea ice anomalies on the winter circulation in CCM3. Part II: direct and indirect components of the response. *J Clim* 17(5):877–889. [https://doi.org/10.1175/1520-0442\(2004\)017<0877:EONAS>2.0.CO;2](https://doi.org/10.1175/1520-0442(2004)017<0877:EONAS>2.0.CO;2)
- Deser C, Hurrell JW, Phillips AS (2017) The role of the north atlantic oscillation in European climate projections. *Clim Dyn* 49(9):3141–3157. <https://doi.org/10.1007/s00382-016-3502-z>
- Dix M, Vohralik P, Bi D, Rashid H, Marsland S, O'Farrell S, Uotila P, Hirst T, Kowalczyk E, Sullivan A et al (2013) The ACCESS Coupled Model: documentation of core CMIP5 simulations and initial results. *Aust Meteorol Oceanogr J* 63(1):83–99. <https://doi.org/10.22499/2.6301.006>
- Donner LJ, Wyman BL, Hemler RS, Horowitz LW, Ming Y, Zhao M, Golaz JC, Ginoux P, Lin S-J, Schwarzkopf MD, Austin J, Alaka G, Cooke WF, Delworth Thomas L, Freidenreich SM, Gordon CT, Griffies SM, Held IM, Hurlin WJ, Klein SA, Knutson TR, Langenhorst AR, Lee H-C, Lin Y, Magi BI, Malyshev SL, Milly PCD,

- Naik V, Nath MJ, Pincus R, Ploshay JJ, Ramaswamy V, Seman CJ, Shevliakova E, Sirutis JJ, Stern WF, Stouffer RJ, Wilson RJ, Winton M, Wittenberg AT, Zeng F (2011) The dynamical core, physical parameterizations, and basic simulation characteristics of the atmospheric component AM3 of the GFDL global coupled model CM3. *J Clim* 24(13):3484–3519. <https://doi.org/10.1175/2011JCLI3955.1>
- Duchon CE (1979) Lanczos filtering in one and two dimensions. *J Appl Meteorol* 18(8):1016–1022. [https://doi.org/10.1175/1520-0450\(1979\)018<1016:LFIOAT>2.0.CO;2](https://doi.org/10.1175/1520-0450(1979)018<1016:LFIOAT>2.0.CO;2)
- Dufresne J-L, Foujols M-A, Denvil S, Caubel A, Marti O, Aumont O, Balkanski Y, Bekki S, Bellenger H, Benshila R, Bony S, Bopp L, Braconnot P, Brockmann P, Cadule P, Cheruy F, Codron F, Cozic A, Cugnet D, de Noblet N, Duvel J-P, Ethé C, Fairhead L, Fichetef T, Flavoni S, Friedlingstein P, Grandpeix J-Y, Guez L, Guilyardi E, Hauglustaine D, Hourdin F, Idelkadi A, Ghattas J, Joussaume S, Kageyama M, Krinner G, Labetoulle S, Lahellec A, Lefebvre M-P, Lefevre F, Levy C, Li ZX, Lloyd J, Lott F, Madec G, Mancip M, Marchand M, Masson S, Meurdesoif Y, Mignot J, Musat I, Parouty S, Polcher J, Rio C, Schulz M, Swingedouw D, Szopa S, Talandier C, Terray P, Viovy N, Vuichard N (2013) Climate change projections using the IPSL-CM5 Earth System Model: from CMIP3 to CMIP5. *Clim Dyn* 40(9):2123–2165. <https://doi.org/10.1007/s00382-012-1636-1>
- Dunne JP, John JG, Adcroft AJ, Griffies SM, Hallberg RW, Shevliakova E, Stouffer Ronald J, Cooke W, Dunne KA, Harrison MJ, Krasting JP, Malyshev SL, Milly PCD, Phillips PJ, Sentman LT, Samuels BL, Spelman MJ, Winton M, Wittenberg AT, Zadeh N (2012) GFDL's ESM2 global coupled climate-carbon earth system models. Part I: Physical formulation and baseline simulation characteristics. *J Clim* 25(19):6646–6665. <https://doi.org/10.1175/JCLI-D-11-00560.1>
- EC (2013) A 2030 framework for climate and energy policies. Tech. rep., European Commission, Brussels, Belgium, <http://eur-lex.europa.eu/legal-content/EN/TXT/?uri=CELEX:52013DC0169>
- Ely CR, Brayshaw DJ, Methven J, Cox J, Pearce O (2013) Implications of the north atlantic oscillation for a uknorway renewable power system. *Energy Policy* 62:1420–1427. <https://doi.org/10.1016/j.enpol.2013.06.037>
- Fogli PG, Manzini E, Vichi M, Alessandri A, Patara L, Gualdi S, Scoccimarro E, Masina S, Navarra A (2009) INGV-CMCC Carbon (ICC): a carbon cycle earth system model. INGV-CMCC, Bologna, Italy. https://is.enes.org/archive-1/archive/documents/CMCC_rp0061-ans-04-2009.pdf
- Giorgetta MA, Manzini E, Roeckner E, Esch M, Bengtsson L (2006) Climatology and forcing of the quasi-biennial oscillation in the MAECHAM5 model. *J Clim* 19(16):3882–3901. <https://doi.org/10.1175/JCLI3830.1>
- Giorgetta MA, Jungclaus J, Reick CH, Legutke S, Bader J, Böttinger M, Brovkin V, Cruieger T, Esch M, Fieg K, Glushak K, Gayler V, Haak H, Hollweg HD, Ilyina T, Kinne S, Kornblueh L, Matei D, Mauritsen T, Mikolajewicz U, Mueller W, Notz D, Pithan F, Raddatz T, Rast S, Redler R, Roeckner E, Schmidt H, Schnur R, Segsneider J, Six KD, Stockhause M, Timmreck C, Wegner J, Widmann H, Wieners K-H, Claussen M, Marotzke J, Stevens B (2013) Climate and carbon cycle changes from 1850 to 2100 in MPI-ESM simulations for the coupled model intercomparison project phase 5. *J Adv model Earth Syst* 5(3):572–597. <https://doi.org/10.1002/jame.20038>
- Gross M, Wan H, Rasch PJ, Caldwell PM, Williamson DL, Klocke D, Jablonowski C, Thatcher DR, Wood N, Cullen M, Beare B, Willett M, Lemari F, Blayo E, Malardel S, Termonia P, Gassmann A, Lauritzen PH, Johansen H, Zarzycki CM, Sakaguchi K, Leung R (2018) Physicsdynamics coupling in weather, climate, and earth system models: challenges and recent progress. *Mon Weather Rev* 146(11):3505–3544. <https://doi.org/10.1175/MWR-D-17-0345.1>
- Hamlington BD, Hamlington PE, Collins SG, Alexander SR, Kim KY (2015) Effects of climate oscillations on wind resource variability in the United States. *Geophys Res Lett* 42(1):145–152. <https://doi.org/10.1002/2014GL062370>
- Hazeleger W, Severijns C, Semmler T, Ștefănescu S, Yang S, Wang X, Wyser K, Dutra E, Baldasano JM, Bintanja R, Bougeault P, Caballero R, Ekman AML, Christensen JH, van den Hurk B, Jones Jimenez PC, Källberg P, Koenigk T, McGrath R, Miranda P, van Noije T, Palmer T, Parodi JA, Schmith T, Selten F, Storelvmo T, Sterl A, Tapamo H, Vancoppenolle M, Viterbo P, Willén U (2010) EC-Earth. *Bull Am Meteorol Soc* 91(10):1357–1364. <https://doi.org/10.1175/2010BAMS2877.1>
- Hazeleger W, Wang X, Severijns C, Ștefănescu S, Bintanja R, Sterl A, Semmler T, Wyser K, Yang S, van den Hurk B, van Noije T, van der Linden E, van der Wiel K (2011) EC-Earth V2.2: description and validation of a new seamless earth system prediction model. *Clim Dyn* 39(11):2611–2629. <https://doi.org/10.1007/s00382-011-1228-5>
- Holtslag AAM, Svensson G, Baas P, Basu S, Beare B, Beljaars ACM, Bosveld FC, Cuxart J, Lindvall J, Steeneveld GJ, Tjernström M, Van De Wiel BJH (2013) Stable atmospheric boundary layers and diurnal cycles: challenges for weather and climate models. *Bull Am Meteorol Soc* 94(11):1691–1706. <https://doi.org/10.1175/BAMS-D-11-00187.1>
- Ji D, Wang L, Feng J, Wu Q, Cheng H, Zhang Q, Yang J, Dong W, Dai Y, Gong D, Zhang R-H, Wang X, Liu J, Moore JC, Chen D, Zhou M (2014) Description and basic evaluation of Beijing Normal University Earth System Model (BNU-ESM) version 1. *Geoscientific Model Dev* 7(5):2039–2064. <https://doi.org/10.5194/gmd-7-2039-2014>
- Jones CD, Hughes JK, Bellouin N, Hardiman SC, Jones GS, Knight J, Liddicoat S, O'Connor FM, Andres RJ, Bell C, Boo K-O, Bozzo A, Butchart N, Cadule P, Corbin KD, Doutriaux-Boucher M, Friedlingstein P, Gornall J, Gray L, Halloran PR, Hurtt G, Ingram WJ, Lamarque J-F, Law RM, Meinshausen M, Osprey S, Palin EJ, Parsons CL, Raddatz T, Sanderson MG, Sellar AA, Schurer A, Valdes P, Wood N, Woodward S, Yoshioka M, Zerroukat M (2011) The HadGEM2-ES implementation of CMIP5 centennial simulations. *Geoscientific Model Dev* 4(3):543–570. <https://doi.org/10.5194/gmd-4-543-2011>
- Karnauskas KB, Lundquist JK, Zhang L (2018) Southward shift of the global wind energy resource under high carbon dioxide emissions. *Nature Geosci* 11:38–43. <https://doi.org/10.1038/s41561-017-0029-9>
- Kröner N, Kotlarski S, Fischer E, Lüthi D, Zubler E, Schär C (2017) Separating climate change signals into thermodynamic, lapse-rate and circulation effects: theory and application to the european summer climate. *Clim Dyn* 48(9):3425–3440. <https://doi.org/10.1007/s00382-016-3276-3>
- Li L, Lin P, Yu Y, Wang B, Zhou T, Liu L, Liu J, Bao Q, Xu S, Huang W, Xia K, Pu Y, Dong L, Shen S, Liu Y, Hu N, Liu M, Sun W, Shi X, Zheng W, Wu B, Song M, Liu H, Zhang X, Wu G, Xue W, Huang X, Yang G, Song Z, Qiao F (2013) The flexible global ocean-atmosphere-land system model, Grid-point Version 2: FGOALS-g2. *Adv Atmos Sci* 30(3):543–560. <https://doi.org/10.1007/s00376-012-2140-6>
- Lindvall J, Svensson G, Hannay C (2013) Evaluation of near-surface parameters in the two versions of the atmospheric model in cesm1 using flux station observations. *J Clim* 26(1):26–44. <https://doi.org/10.1175/JCLI-D-12-00020.1>
- Lindvall J, Svensson G, Caballero R (2017) The impact of changes in parameterizations of surface drag and vertical diffusion on the large-scale circulation in the community atmosphere model (CAM5). *Clim Dyn* 48(11):3741–3758. <https://doi.org/10.1007/s00382-016-3299-9>

- Ma J, Foltz GR, Soden BJ, Huang G, He J, Dong C (2016) Will surface winds weaken in response to global warming? *Environ Res Lett* 11(12):124012. <http://stacks.iop.org/1748-9326/11/i=12/a=124012>
- Manzini E, Giorgetta MA, Esch M, Kornbluh L, Roeckner E (2006) The influence of sea surface temperatures on the northern winter stratosphere: ensemble simulations with the MAECHAM5 model. *J Clim* 19(16):3863–3881. <https://doi.org/10.1175/JCLI3826.1>
- North GR, Bell TL, Cahalan RF, Moeng FJ (1982) Sampling errors in the estimation of empirical orthogonal functions. *Mon Weather Rev* 110(7):699–706. [https://doi.org/10.1175/1520-0493\(1982\)110<0699:SEITEO>2.0.CO;2](https://doi.org/10.1175/1520-0493(1982)110<0699:SEITEO>2.0.CO;2)
- Pryor SC, Schoof JT, Barthelmie RJ (2006) Winds of change?: Projections of near-surface winds under climate change scenarios. *Geophys Res Lett*. <https://doi.org/10.1029/2006GL026000>
- Reyers M, Moemken J, Pinto JG (2016) Future changes of wind energy potentials over Europe in a large CMIP5 multi-model ensemble. *Int J Climatol* 36(2):783–796. <https://doi.org/10.1002/joc.4382>
- Rotstayn LD, Jeffrey SJ, Collier MA, Dravitzki SM, Hirst AC, Syktus JJ, Wong KK (2012) Aerosol- and greenhouse gas-induced changes in summer rainfall and circulation in the Australasian region: a study using single-forcing climate simulations. *Atmos Chem Phys* 12(14):6377–6404. <https://doi.org/10.5194/acp-12-6377-2012>
- Scoccimarro E, Gualdi S, Bellucci A, Sanna A, Giuseppe FP, Manzini E, Vichi M, Oddo P, Navarra A (2011) Effects of tropical cyclones on ocean heat transport in a high-resolution coupled general circulation model. *J Clim* 24(16):4368–4384. <https://doi.org/10.1175/2011JCLI4104.1>
- Shepherd T (2014) Atmospheric circulation as a source of uncertainty in climate change projections. *Nat Geosci* 7:703–708. <https://doi.org/10.1038/ngeo2253>
- Shin HH, Ming Y, Zhao M, Golaz JC, Xiang B, Guo H (2018) Evaluation of planetary boundary layer simulation in GFDL atmospheric general circulation models. *J Clim* 31(13):5071–5087. <https://doi.org/10.1175/JCLI-D-17-0543.1>
- Simpson IR, Shaw TA, Seager R (2014) A diagnosis of the seasonally and longitudinally varying midlatitude circulation response to global warming. *J Atmos Sci* 71(7):2489–2515. <https://doi.org/10.1175/JAS-D-13-0325.1>
- Taylor KE, Stouffer RJ, Meehl GA (2012) An overview of CMIP5 and the experiment design. *Bull Am Meteorol Soc* 93(4):485–498. <https://doi.org/10.1175/BAMS-D-11-00094.1>
- Tjiputra JF, Olsen A, Assmann K, Pfeil B, Heinze C (2012) A model study of the seasonal and long-term North Atlantic surface pCO₂ variability. *Biogeosciences* 9(3):907–923. <https://doi.org/10.5194/bg-9-907-2012>
- Tobin I, Vautard R, Balog I, Bréon FM, Jerez S, Ruti PM, Thais F, Vrac M, Yiou P (2015) Assessing climate change impacts on European wind energy from ensembles high-resolution climate projections. *Clim Change* 128(1):99–112. <https://doi.org/10.1007/s10584-014-1291-0>
- Tobin I, Jerez S, Vautard R, Thais F, van Meijgaard E, Prein A, Déqué M, Kotlarski S, Maule CF, Nikulin G, Nol T, Teichmann C (2016) Climate change impacts on the power generation potential of a European mid-century wind farms scenario. *Env Res Lett* 11(3):034013. <http://stacks.iop.org/1748-9326/11/i=3/a=034013>
- Torralba V, Doblas-Reyes FJ, Gonzalez-Reviriego N (2017) Uncertainty in recent near-surface wind speed trends: a global reanalysis intercomparison. *Env Res Lett* 12(11):114019. <http://stacks.iop.org/1748-9326/12/i=11/a=114019>
- Ulbrich U, Leckebusch GC, Pinto JG (2009) Extra-tropical cyclones in the present and future climate: a review. *Theor Appl Climatol* 96(1):117–131. <https://doi.org/10.1007/s00704-008-0083-8>
- Vautard R, Cattiaux J, Yiou P, Thépaut JN, Ciais P (2010) Northern hemisphere atmospheric stilling partly attributed to an increase in surface roughness. *Nature Geosci* 3:756–761. <https://doi.org/10.1038/ngeo979>
- Volodin EM, Dianskii NA, Gusev AV (2010) Simulating present-day climate with the INMCM4.0 coupled model of the atmospheric and oceanic general circulations. *Izvestiya Atmos Oceanic Phys* 46(4):414–431. <https://doi.org/10.1134/S000143381004002X>
- Watanabe S, Hajima T, Sudo K, Nagashima T, Takemura T, Okajima H, Nozawa T, Kawase H, Abe M, Yokohata T, Ise T, Sato H, Kato E, Takata K, Emori S, Kawamiya M (2011) MIROC-ESM 2010: model description and basic results of CMIP5-20c3m experiments. *Geoscientific Model Dev* 4(4):845–872. <https://doi.org/10.5194/gmd-4-845-2011>
- WindEurope (2018) Wind in power 2017. In: Annual combined onshore and offshore wind energy statistics. Tech. rep., Wind-Europe, Brussels, Belgium. <https://windeurope.org/about-wind/statistics/european/wind-in-power-2017/>
- Wohland J, Reyers M, Weber J, Witthaut D (2017) More homogeneous wind conditions under strong climate change decrease the potential for inter-state balancing of electricity in Europe. *Earth Syst Dyn* 8(4):1047–1060. <https://doi.org/10.5194/esd-8-1047-2017>
- Wu T, Song L, Li W, Wang Z, Zhang H, Xin X, Zhang Y, Zhang L, Li J, Wu F, Liu Y, Zhang F, Shi X, Chu M, Zhang J, Fang Y, Wang F, Lu Y, Liu X, Wei M, Liu Q, Zhou W, Dong M, Zhao Q, Ji J, Li L, Zhou M (2014) An overview of BCC climate system model development and application for climate change studies. *J Meteorol Res* 28(1):34–56. <https://doi.org/10.1007/s13351-014-3041-7>
- Yukimoto S, Adachi T, Hosaka M, Sakami T, Yoshimura H, Hirabara M, Tanaka TY, Shindo E, Tsujino H, Deushi M, Mizuta R, Yabu S, Obata A, Nakano H, Koshiro T, Ose T, Kitoh A (2012) A new global climate model of the meteorological research institute: MRI-CGCM3—Model description and basic performance. *J Meteorol Soc Jpn Ser II* 90A:23–64. <https://doi.org/10.2151/jmsj.2012-A02>
- Zappa G, Shepherd TG (2017) Storylines of atmospheric circulation change for European regional climate impact assessment. *J Clim* 30(16):6561–6577. <https://doi.org/10.1175/JCLI-D-16-0807.1>
- Zappa G, Hoskins BJ, Shepherd TG (2015a) The dependence of wintertime Mediterranean precipitation on the atmospheric circulation response to climate change. *Env Res Lett* 10(10):104012. <http://stacks.iop.org/1748-9326/10/i=10/a=104012>
- Zappa G, Hoskins BJ, Shepherd TG (2015b) Improving climate change detection through optimal seasonal averaging: the case of the North Atlantic jet and European precipitation. *J Clim* 28(16):6381–6397. <https://doi.org/10.1175/JCLI-D-14-00823.1>
- Zappa G, Pithan F, Shepherd TG (2018) Multimodel evidence for an atmospheric circulation response to Arctic sea ice loss in the CMIP5 future projections. *Geophys Res Lett* 45(2):1011–1019. <https://doi.org/10.1002/2017GL076096>
- Zubiate L, McDermott F, Sweeney C, O'Malley M (2017) Spatial variability in winter near-wind speed relationships in western Europe linked to concomitant states of the east Atlantic and Scandinavian patterns. *Q J R Meteorol Soc* 143(702):552–562. <https://doi.org/10.1002/qj.2943>

Publisher's Note Springer Nature remains neutral with regard to jurisdictional claims in published maps and institutional affiliations